JOC*Article*

Solid-State Reaction Mechanisms in Monomer−Dimer Interconversions of *p*-Bromonitrosobenzene. Single-Crystal-to-Single-Crystal Photodissociation and Formation of New Non-van der Waals Close Contacts

Ivan Halasz, Ernest Mestrovic, Helena Cicak, Zlatko Mihalic, and Hrvoj Vancik*

Department of Chemistry, Faculty of Science and Mathematics, University of Zagreb, Horvatovac 102A, 10000 Zagreb, Croatia

vancik@irb.hr

Received June 16, 2005

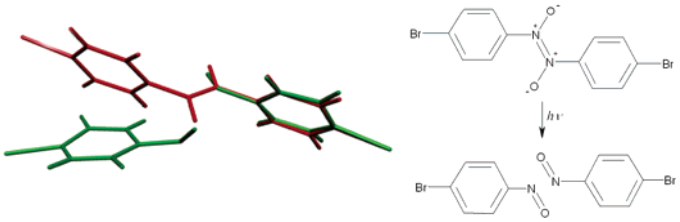

Thermal and photochemical reactions and the phase transition mechanisms of solid-state monomer−dimer interconversions of *p*-bromonitrosobenzene were studied on the basis of kinetics data and single-crystal-to-single-crystal transformations. From the crystal structure and packing of *p*-bromobenzeneazodioxide and the previously determined structure of the freshly sublimed monomer, we have explained both consecutive steps in thermal dimerization. While the first reaction (formation of the metastable dimer) with first-order kinetics affords diminishing of the (*2 2 0*) *critical crystal plane* that intersects atoms of the nitroso groups, the second phase transformation step includes *four critical planes*, which show sigmoid kinetics. In the new phase growth, these crystal planes developed in two (Cartesian) dimensions as vectors perpendicular to *ab* and *ac* planes, which is in agreement with the dimensionality previously determined on the basis of the Avrami−Erofeyev analysis (with $m = 2.01$). Photochromic dissociation of the azodioxide at 100 K was followed by structure determination of the single-crystal-to-single-crystal transformation. A new metastable monomer was discovered, in which, despite bond breaking, the nitrogen atoms of the neighboring monomers remained very close to each other (2.30 Å), i.e., 23.3% closer than is the sum of two N-atom van der Waals radii. Such an extraordinary close contact was also observed between N and O atoms. This tight packing can explain why the return to dimerization after the low temperature photodissociation occurs so rapidly at a temperature as low as 170 K.

Introduction

Chemical reactions in the solid state are in different ways more or less accompanied and coupled with phase changes in the crystal lattice.[1] Since both processes, i.e., change in covalent topology (chemical reaction) and conversion of supramolecular self-organization (e.g., phase transformation), occur in more or less rigid condensed systems, our concept of the reaction mechanism must be extended in such a way that it includes both processes.

The most developed methods for kinetic studies of solid-state reactions are based on thermal analysis (TA).[2] Experimental kinetic curves were explained on the basis of their fitting different theoretical models, such as the Avrami−Erofeyev or Prout-Tomkins and Skrdla models, etc.[3] The obtained TA results were mostly used to explain the phase transformation mechanisms, for instance, in terms of the dimensionality (Cartesian) of the new phase growth.

The disadvantage of methods based only on the TA kinetics is their being based more on pure phenomenology than on the molecularity of the mechanism.[4] It is much

(1) Schmidt, G. M. J. et al. *Solid State Photochemistry*; Ginsburg, D., Ed.; Verlag Chemie: Weinheim, New York, 1976; p 80.

(2) Brown, M. E.; Dollimore, D.; Galwey, A. K. *Comprehensive Chemical Kinetics*; Elsevier: Amsterdam, 1980; Vol. 22.
(3) Skrdla, P. J. *J. Phys. Chem. A* **2004**, *108*, 6709−6712.
(4) Galwey, A. K. *Thermochim. Acta* **2004**, *413*, 139−183.

10.1021/jo051236u CCC: $30.25
Published on Web 09/17/2005

SCHEME 1

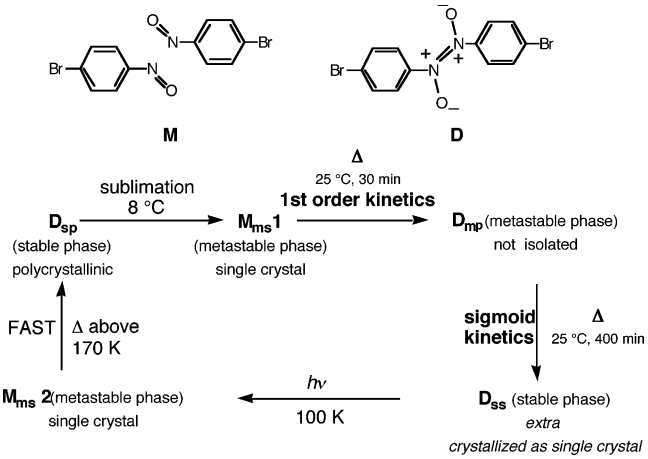

more informative when the solid-state reaction mechanism and its relation to the reaction and/or phase change kinetics is based on a combination of the TR-XRPD methods and spectroscopy. To find out how a solid-state chemical reaction and phase conversion are coupled, it is appropriate to measure the chemical process and the corresponding phase changes by different and independent experimental methods. Whereas the rate of chemical reaction can be best determined by spectroscopy by following the change in concentration of the product or the reactant with time, the solid-state phase transition kinetics can be well studied by time-resolved X-ray powder diffraction methods (TR-XRPD).[5] If the crystal structures of reactants, products, and perhaps intermediates (metastable polymorphs) are known, then we can get a deeper insight into the molecularity of the chemical change and its reflection on the kinetic behavior.

In our recent paper[6] we applied such an approach and found that the thermal solid-state dimerization of substituted nitrosobenzenes can be a good model for such mechanistic studies.

We found that freshly sublimed *p*-bromonitrosobenzene **M** undergoes dimerization to the corresponding azodioxide **D** (Scheme 1). This solid-state transformation consists of two consecutive processes, the chemical reaction coupled with nucleation, expressing a first-order kinetics, and a consecutive sigmoid phase transition from the metastable to the stable product phase.[6a] The likelihood of the first process has been explained on the basis of the disordered crystal structure of monomer **M**.[6b] Also it has been found that this first-order kinetics curve corresponds to the disappearance of the powder X-ray diffraction peak at 2Θ = 27.5 °, which was assigned to the (*2 0 0*) crystal plane (we called it *critical crystal plane)* that intersects N and O atoms of the nitroso groups. The second consecutive process with the sigmoid kinetic curve was measured for the diffraction peak at 2Θ = 25.8 °. However, since the crystal structure of the dimeric product (**D** in Scheme 1) was not known at the time, we were not able to determine to which crystal plane (or ensemble of planes) belongs the X-ray diffraction peak at 2Θ = 25.8 ° showing this sigmoid kinetics.

In one of our previous papers[7] we also demonstrated that azodioxides such as **D** show photochromic dissociation to nitroso monomers in the solid state under cryogenic conditions (10−100 K). However, the obtained nitroso monomers cannot survive a temperature much higher than 170 K and dimerize so quickly that it was not possible to measure this reaction rate. Evidently, such a low-temperature photoproduct turns up as a metastable polymorph of the monomer.

In summary, the overall photo- and thermochemical monomer−dimer behavior of the solid *p*-bromonitrosobenzene can be represented by Scheme 1.

Sublimation of the crude polycrystalline dimer $\mathbf{D_{sp}}$ on the coldfinger of the sublimator precooled to 8 °C yields metastable single crystals of monomer $\mathbf{M_{ms}1}$, whose structure was determined by X-ray diffraction on the single crystal. Two processes, the 30 min long dimerization with first-order nucleation kinetics that yields the dimer in the metastable phase $\mathbf{D_{mp}}$, followed by a 400 min long phase transformation with sigmoid kinetics, led to the stable dimeric phase $\mathbf{D_{ss}}$.

In this work, we will try to answer two questions: (i) why the solid state $\mathbf{M} \rightarrow \mathbf{D}$ dimerization is so slow if we start with the freshly sublimed monomer $\mathbf{M_{ms}1}$ as compared to the fast dimerization of monomer $\mathbf{M_{ms}2}$ that was obtained by the low-temperature photolysis of dimer $\mathbf{D_{ss}}$, and (ii) which is the critical crystal plane (or ensemble of planes) that affords sigmoid kinetics in the $\mathbf{D_{mp}} \rightarrow \mathbf{D_{ss}}$ phase transition.

Results and Discussion

Single-Crystal-to-Single-Crystal Photolysis. To answer these questions, we first determined the crystal structure of the stable polymorph $\mathbf{D_{ss}}$ and then analyzed the structural changes that appear in the single-crystal-to-single-crystal transformation during the low-temperature photodissociation of azodioxide $\mathbf{D_{ss}}$ to the nitroso monomer, i.e., its polymorph $\mathbf{M_{ms}2}$.

Independently of how $\mathbf{D_{ss}}$ is obtained, by sublimation and phase transformation (through the metastable species $\mathbf{M_{ms}1}$ and $\mathbf{D_{mp}}$) or after these processes crystallize from methylene dichloride, it belongs to the same crystal phase. The powder diffractogram calculated on the basis of the crystal structure of the single crystal $\mathbf{D_{ss}}$ matches the powder diffractogram recorded before crystallization for crude $\mathbf{D_{ss}}$.

Applying crystallization from solution, we have prepared the stable single crystal of dimer $\mathbf{D_{ss}}$ and photolyzed it by UV light in an X-ray diffractometer at 100 K. After 9 h of irradiation, the color of the crystal changed from colorless to blue. As we have shown previously by FT-IR spectroscopy (see ref 7 and S1 Appendix in its Supporting Information), since the 1665 cm^{-1} signal of the azodioxide (ON═NO) group of the dimer disappears completely after 1 h of irradiation under the same photolytical conditions, we believe that after 9 h of irradiation there is complete or almost complete conver-

(5) Kim, J. H.; Hubig, S. M.; Lindeman, S. U.; Kochi, J. K. *J. Am. Chem. Soc.* **2001**, *123*, 87−95.

(6) (a) Vancik, H.; Simunic-Meznaric, V.; Mestrovic, E.; Halasz, I. *J. Org. Chem.* **2004**, *69*, 4829−4834. (b) In a previous paper[6a] we explained that only the first step (producing $\mathbf{M_{ms}1}$) of the reaction could convert to 50%. However, the complete thermal reaction that includes also a long period of the phase transformation led to the complete dimerization.

(7) Vancik, H.; Simunic-Meznaric, V.; Caleta, I.; Mestrovic, E.; Milovac, S.; Mlinaric Majerski, K.; Veljkovic, J. *J. Phys. Chem. B* **2002**, *106*, 1576−1580.

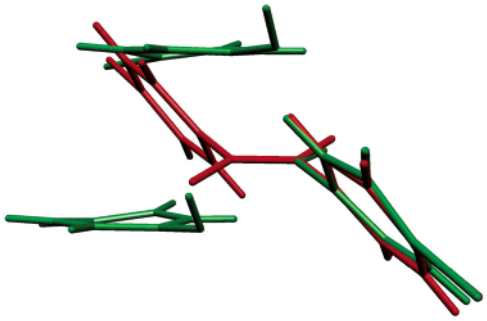

FIGURE 1. Superposition of the dimer molecules of $\mathbf{D_{ss}}$ (red) and the product monomers $\mathbf{M_{ms}2}$ (green) after the single-crystal-to-single-crystal photodissociation.

sion of dimer to monomer. The quality of the reactant and the photoproduct single crystals at 100 K was good enough for resolving both structures. We found that the single crystal of the photoproduct was the nitroso monomer in the second metastable phase, $\mathbf{M_{ms}2}$, which by warming above 170 K quickly converts to the stable polycrystalline dimer $\mathbf{D_{sp}}$. In this way, the complete reaction cycle of the solid-state monomer dimer conversions of the *p*-bromonitrosobenzene was closed (Scheme 1). Additionally, it must be mentioned that, given the disorder in $\mathbf{M_{ms}1}$, the cyclic mechanism of Scheme 1 should lead to ordered and disordered phases of $\mathbf{M_{ms}2}$ depending on whether one starts with sublimed $\mathbf{M_{ms}1}$ or $\mathbf{D_{ss}}$.

Photodissociation of the crystallized $\mathbf{D_{ss}}$, for which the single-crystal-to-single-crystal conversion was observed, led to the formation of the new metastable polymorph of the monomer, $\mathbf{M_{ms}2}$. Although molecular orientations changed markedly during the reaction (Figure 1), the crystal retained its quality, which was not perfect, as required for typical crystallography research, but quite satisfactory for structure determination necessary for this reaction mechanism study. In general, analysis of single-crystal-to-single-crystal transformation is limited and difficult, especially in this case when thickness of the crystal was only 0.013 mm.

Both dimer $\mathbf{D_{ss}}$ and monomer $\mathbf{M_{ms}2}$ crystallize in the monoclinic crystal system. Unit cells of the compounds differ only in one parameter, i.e., the *a* axis, which in the monomer phase is half the length of that in the dimer phase (Figures 2 and 3). Differences in other cell parameters are so small that they could be attributed to the loss of the crystal quality due to the transformation.

The small decrease in crystal quality can be explained by the fact that, using the same conditions of indexing, almost all (∼98%) of the dimer phase diffraction peaks could be indexed, whereas only approximately half of them could be indexed for the monomer phase. Reflections of the monomer phase started to spread over a significant number of diffraction images, but it was also noted that all of the unindexed reflections were lying in the (*a**,*b**) plane of the reciprocal space. This indicates that structural changes occur only in the (*a*,*b*) plane of the direct space with no movement of the molecules parallel to the *c* axis. Also, as can be seen in the crystal structure of the dimer phase, the two-dimensional networks of the hydrogen bond are parallel to this plane.

In the molecular structure of the $\mathbf{D_{ss}}$ dimer molecule, the benzene rings are parallel but do not lie in the same plane (Figure 4). Atoms of the azodioxy group lie in the same plane (the molecule lies on the inversion center) with the torsional angle ∠(C2−C1−N−O) is 59.1(7)° (Figure 4, green structures). A possible reason for such conformation could be the stabilization of the crystal structure by the two-dimensional framework of C−H···O hydrogen bonds. Assuming that the atoms involved in these interactions do not move significantly during the transformation, then it could be said that these interac-

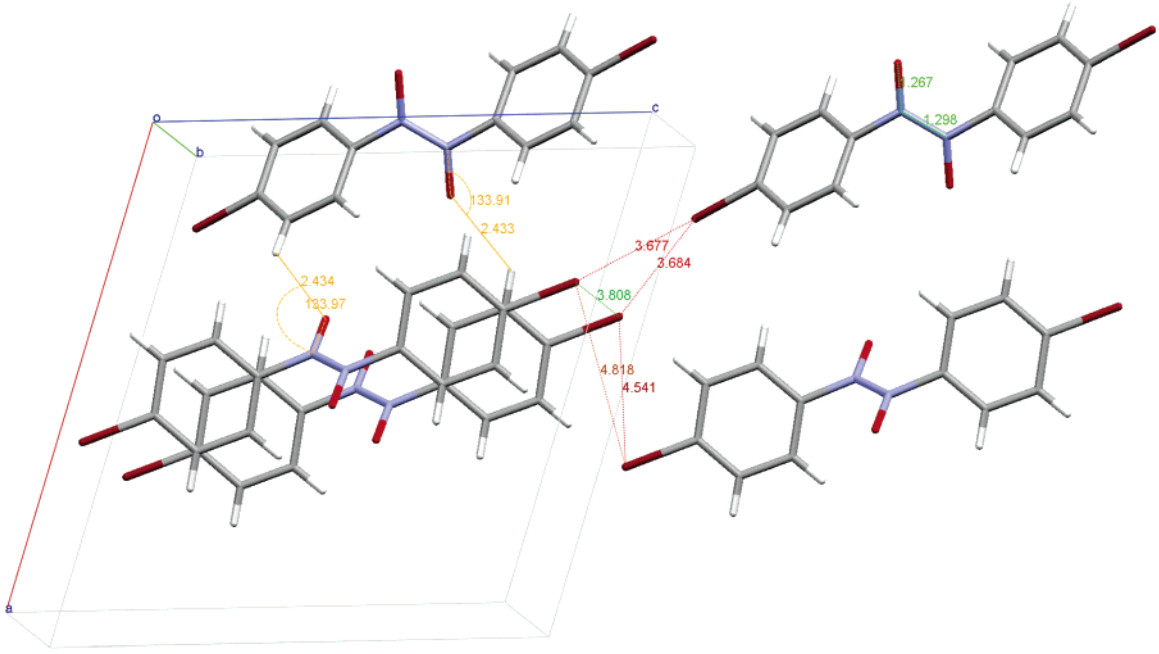

FIGURE 2. Crystal structure and packing of the stable dimer, $\mathbf{D_{ss}}$. The hydrogen bonding network is marked by yellow lines, and bromine−bromine close connections are shown by red lines.

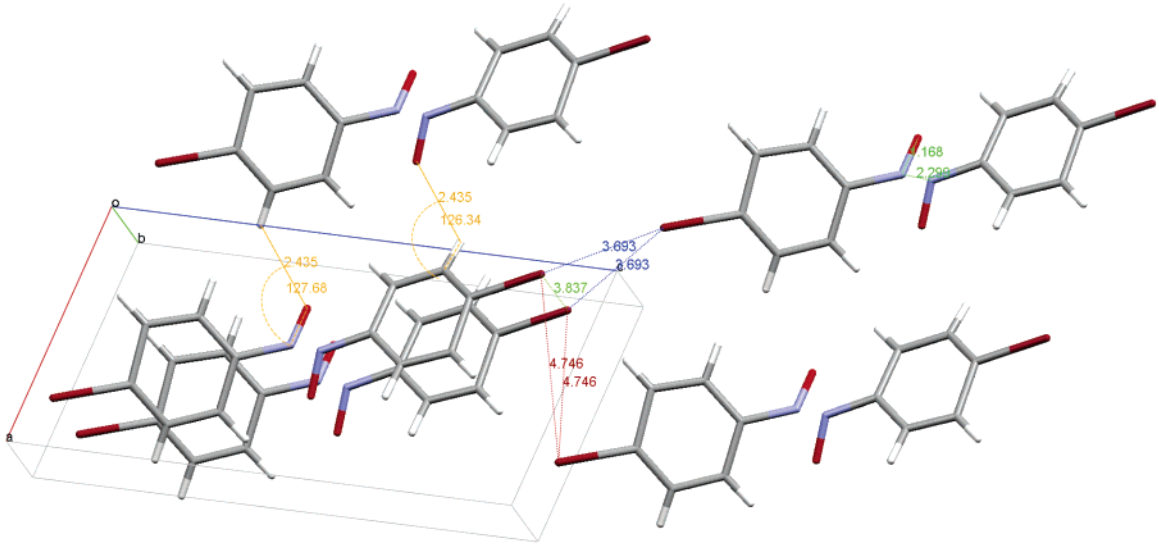

FIGURE 3. Crystal structure and packing of the metastable monomer, $\mathbf{M_{ms}2}$, obtained after photolytic single-crystal-to-single-crystal conversion at 100 K. Hydrogen bonding network is shown by yellow lines, and bromine−bromine close connections are marked by red lines.

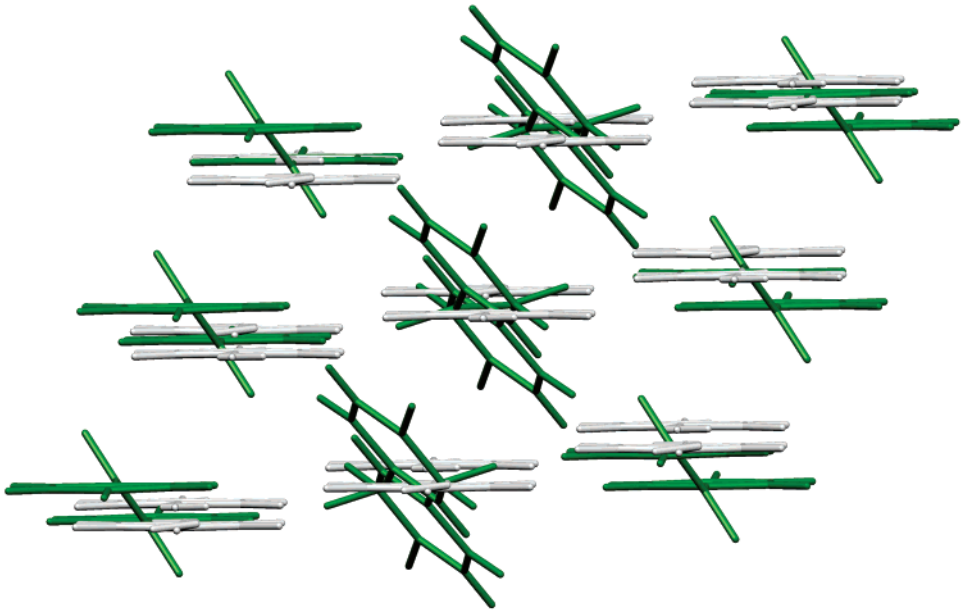

FIGURE 4. Superposition of crystal packing of the sublimed monomer $\mathbf{M_{ms}1}$ (gray) and the stable dimer $\mathbf{D_{ss}}$ (green).

tions govern the route of the transformation (Figures 2 and 3). Analogous crystal packing was observed in all known crystal structures of *p*- and *m*-halogen-substituted azodioxybenzenes. In the monomer $\mathbf{M_{ms}2}$ phase, this (C2−C1−N−O) torsional angle is 46.2(2.4)°. It might be expected that the energetically most favorable conformation of the monomer molecule would be the one in which the nitroso group is in plane with the benzene ring. However, this would leave hydrogen bonds weaker. This assumption is supported by the crystal structure of *p*-iodonitrosobenzene,[8] which exists as a stable monomer and in which the corresponding torsion angle is close to zero.

As can be seen from Figures 2 and 3, not only hydrogen bonds but also the Br···Br interactions network remain conserved during the chemical reaction. The geometrical parameters of these interactions do not change significantly; they are almost within the estimated standard deviations.

On the other hand, the N···N distance greatly increases upon the $\mathbf{D_{ss}} \rightarrow \mathbf{M_{ms}2}$ transformation from 1.30 Å in the monomer phase to 2.30 Å in the dimer phase. Since this N=N bond is broken during the photodissociation, such a change, as commented bellow, could be expected.

Mechanism of the $\mathbf{D_{mp}}$ to $\mathbf{D_{ss}}$ Transition. Since we know the crystal structures of the crucial points of the reaction cycle in Scheme 1, i.e., structures of $\mathbf{M_{ms}1}$, $\mathbf{D_{ss}}$, and $\mathbf{M_{ms}2}$, we can discuss the solid-state reaction mechanisms of monomer−dimer interconversions in more detail.

Let us first discuss the mechanisms of the $\mathbf{M_{ms}1} \rightarrow \mathbf{D_{mp}} \rightarrow \mathbf{D_{ss}}$ transformation. Two important geometrical changes

(8) (a) Webster, M. S. *J. Chem. Soc.* **1956**, 2841. (b) Talberg, H. J. *Acta Chem. Scand. A* **1979**, *33*, 289.

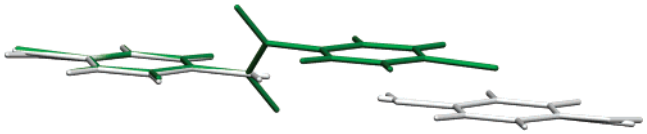

FIGURE 5. Superposition of crystal structures of the sublimed monomer $\mathbf{M_{ms}1}$ (gray) and the stable dimer $\mathbf{D_{ss}}$ (green). Monomer molecules are 50% disordered (see ref 6).

can be recognized from the superposition of the crystal packing of $\mathbf{M_{ms}1}$ and $\mathbf{D_{ss}}$ (Figure 4). While the first change includes the declination of the nitroso groups plane out of the benzene rings plane, the second change is the inclination of every second dimeric molecule and the formation of a new packing plane. Marked differences in packing between $\mathbf{M_{ms}1}$ and $\mathbf{D_{ss}}$ could be a satisfactory explanation for the relatively slow two-step process of the stable dimer $\mathbf{D_{ss}}$ formation. At the molecular level, dimerization requires two spatial shifts, the monomer molecule $\mathbf{M_{ms}1}$ (gray structure in Figure 5) must be shifted in two directions, horizontally in the benzene ring plane, but also vertically to this plane (Figure 5).

Perhaps one could speculate that these two changes correspond to the "trajectories" associated with two consecutive processes, the chemical reaction ($\mathbf{M_{ms}1} \rightarrow \mathbf{D_{mp}}$) that afforded first-order kinetics and the phase transfer from $\mathbf{D_{mp}}$ to $\mathbf{D_{ss}}$ with sigmoid kinetics. We found previously that in the $\mathbf{M_{ms}1} \rightarrow \mathbf{D_{mp}}$ process the first-order kinetics mostly shows a disappearance of the diffraction peak of the (*2 0 0*) crystal plane (critical crystal plane) where the nitroso group is positioned. To find such a critical plane for the second process, the 400 min long $\mathbf{D_{mp}} \rightarrow \mathbf{D_{ss}}$ phase transformation characterized by sigmoid kinetics, we must look at the crystal packing of product $\mathbf{D_{ss}}$. The strongest sigmoid growth recorded by the TR-XRPD shows the diffraction peak at $2\Theta = 25.8$ °. On the basis of the crystal structure of $\mathbf{D_{ss}}$, we assigned this peak to a superposition of four diffraction peaks corresponding to crystal planes (*0 1 2*), (*1 1 2*), (*2 1 0*), and (*10-4*). The position of these planes relative to the crystal packing of $\mathbf{D_{ss}}$ is shown in Figure 6.

One can observe that three of the planes [(*0 1 2*), (*1 1 2*), (*2 1 0*)] are parallel or nearly parallel with the *ac* plane of the unit cell, whereas the (*10-4*) plane is parallel with the *ab* plane. There is no plane parallel with *bc* of the unit cell. If the directions of the new phase development is described as vectors perpendicular to these four planes (nearly parallel to two planes, *ab* and *ac*, respectively), this phase growth is defined by four vectors distributed more or less in two (Cartesian) dimensions. The previously measured Avrami−Erofeyev parameter *m* was 2.01,[6] which indicates an almost two-dimensional growth. This finding can now be confirmed on the basis of the crystal structure determination. Perhaps, it would be more convenient to describe a new phase growth *multidimensionally*, i.e., in terms of the number of critical crystal planes and the orientation of their growth vectors (perpendicular to these planes) rather than in terms of *Cartesian* three-dimensionality. Thus, our example becomes a four-dimensional problem because the phase growth includes four critical planes. It must be added that because we were not able to deconvolute these four critical planes and to record kinetic curves of each plane

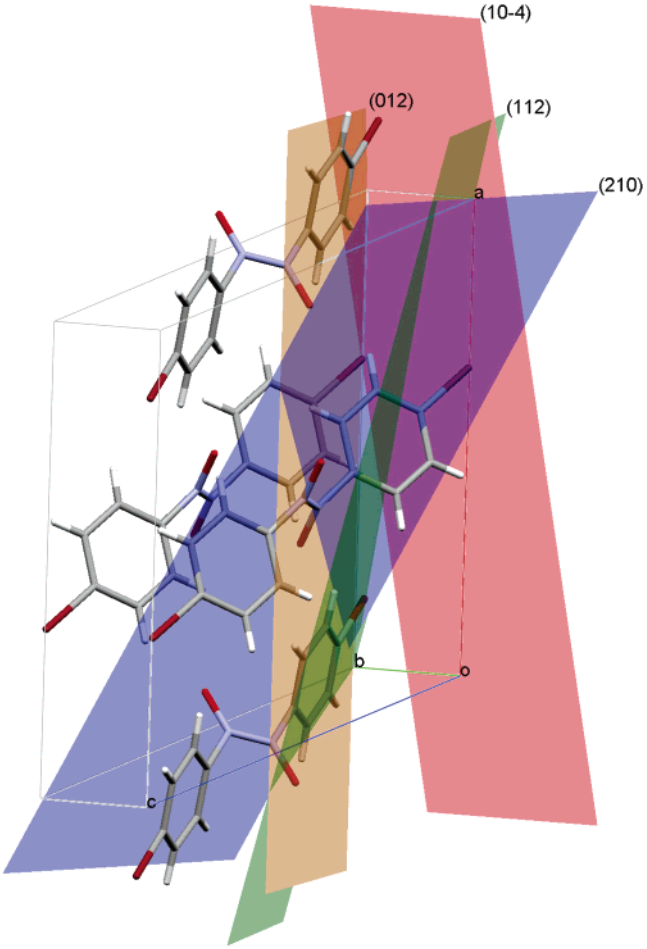

FIGURE 6. Crystal planes of the $\mathbf{D_{ss}}$ single-crystal assigned to X-ray diffraction peaks, which afford sigmoid kinetics, observed for the $\mathbf{D_{mp}} \rightarrow \mathbf{D_{ss}}$ phase transition.

extra, in this moment we do not know to which extent particular planes contribute to the observed kinetics.

Non-van der Waals Close Contacts. Since we have succeeded in observing the single-crystal-to-single-crystal $\mathbf{D_{ss}} \rightarrow \mathbf{M_{ms}2}$ transformation, we were also interested in studying close contacts in more detail by looking at changes in the charge distribution and electron (charge) densities in close contact regions. Starting from the experimentally determined geometry, we have calculated the electron (charge) density surfaces for fragments of three crystal-packed molecules of dimer $\mathbf{D_{ss}}$ (Figure 7a and c) and six crystal-packed molecules of monomer $\mathbf{M_{ms}2}$ (Figure 7b and d).

The non-zero electron density can be observed in the positions of hydrogen bonds between *m*-CH groups of the benzene ring and oxygens of nitroso groups (or azodioxide groups in dimers). It is, however, more interesting to note that a relatively high charge density remains between photochemically disconnected nitrogen atoms in monomers (Figure 7d). The NN distance of 2.30 Å is much shorter than the sum of two nitrogen van der Waals radii (3.0 Å). This shortening amounts to 23.3%, i.e., evidently larger than corresponding shortening observed in the formation of hydrogen bonds (10−15%).[9a] Until now, the shortest NN close contact known from literature is 2.62 Å.[9b] Accordingly, the non-van der Waals NN close con-

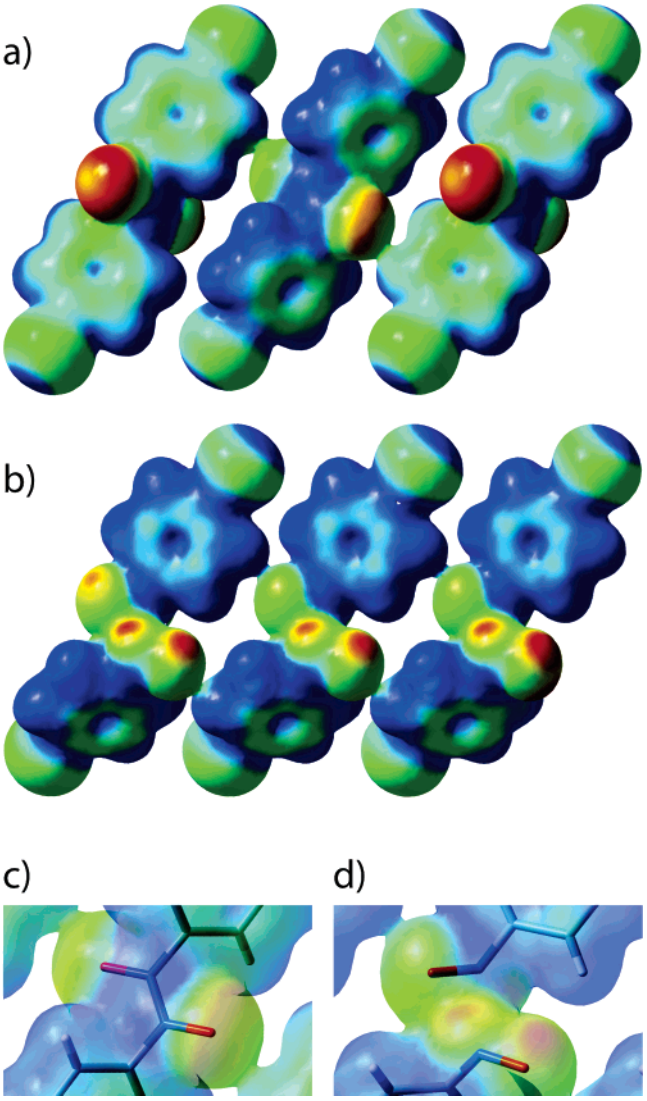

FIGURE 7. Electrostatic potential mapped on the total electron density (isosurface value = 0.0080 au) of (a) sequence of three *p*-bromonitrosobenzene dimeres; (b) sequence of six *p*-bromonitrosobenzenes; (c and d) details in the region of N=N bond, before (c) and after (d) photolysis. Calculations were based on the crystal structure geometry.

SCHEME 2

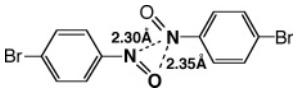

tacts exist in the $\mathbf{M_{ms}2}$ crystal packing. A similar extraordinary close contact, 2.35 Å, is also found between the same nitrogen atom of one monomer and the nitroso oxygen atom of the neighboring molecule. In this way, a three-centric close contact is formed (Scheme 2). Ab initio calculations indicate that the two-molecule complex as the one in Scheme 2 is not persistent in the gas phase; two monomer molecules just dislocate from each other. This means that such close contacts are possible only inside a close crystal packing. The appearance of such structures after photolysis of the solid azodioxide **D** can easily explain why the $\mathbf{M_{ms}2}$ polymorph returns so quickly to the dimer at a temperature as low as 170 K.

On the suggestion of a referee, we have to be very careful when observing an extraordinary shortening and/or lengthening of interatomic distances in crystals. For the so-called bond-stretch isomers,[9c] it was proposed rather to be an epiphenomenon caused by compositional disorder.[9d] However, since we have shown by spectroscopy[7] (vide supra) that photoconversion already is complete after 45 min, it is difficult to believe in the posibility of compositional disorder in the 9 h irradiated single crystal. In his criticism of the bond-stretch isomer phenomenon, Parkin[9d] found that while a small impurity that possesses a molecule with a *long interatomic distance* drastically "stretches" the observed bond length of the main constituent in the crystal, a small impurity of the constituent with *short interatomic distance* has almost no influence on the possible observation of shortening of long interatomic distances. In our case we observed not stretched but squeezed N,N distance, and in accordance with Parkin's observations, even if the crystal after photolysis contains small amounts of the unreacted dimer (which has short N,N distances), it cannot be cause of our observation of short contacts.

Conclusions

From the crystal structure and packing of *p*-bromobenzeneazodioxide **D** and the previously determined structure of the freshly sublimed monomer $\mathbf{M_{ms}1}$, we can explain the solid-state reaction mechanism of both consecutive steps in their thermal conversion. Whereas in the first paper we explained the first reaction (formation of the metastable dimer $\mathbf{D_{mp}}$) as first-order kinetics that affords diminishing of the (*2 2 0*) critical crystal plane intersecting atoms of the nitroso groups, here we found *four critical planes* that show sigmoid kinetics of the second phase transformation step. In the new phase growth these crystal planes develop in two (Cartesian) dimensions as vectors perpendicular to the *ab* and *ac* planes, respectively. This finding is in agreement with the dimensionality previously determined on the basis of the Avrami−Erofeyev analysis (with $m = 2.01$).

Photochromic dissociation of the azodioxide $\mathbf{D_{ss}}$ at 100 K was followed by structure determination of the single-crystal-to-single-crystal transformation. A new metastable monomer $\mathbf{M_{ms}2}$ was discovered in which, despite bond breaking, the nitrogen atoms of the neighboring monomers remained very close to each other (2.30 Å), i.e., 23.3% closer than the sum of two N-atom van der Waals radii. Such an extraordinary close contact is also observed between N and O atoms. Such tight packing can explain why the dimerization after the low temperature photodissociation occurs so quickly at a temperature as low as 170 K.

Experimental Section

p-Bromonitrosobenzene was prepared by standard procedure described in previous literature (ref 6 and references therein).

Crystal Preparation. Numerous experiments were performed with different starting concentrations of the dimer. All

(9) (a) Desiraju, G. R. *Crystal Engineering. The Design of Organic Solids*; Elsevier: Amsterdam, 1989; pp 92, 144. (b) Capiomont, A.; Chion, B.; Lajzerowicz, J. *Acta Crystallogr., Sect. B* **1971**, *27*, 322. (c) Yoon, K.; Parkin, G.; Rheingold, A. L. *J. Am. Chem. Soc.* **1991**, *113*, 1437−1438. (d) Parkin, G. *Acc. Chem. Res.* **1992**, *25*, 455−460.

experiments gave similar results. From these experiments it appears that the rate of evaporation of CH_2Cl_2 is a factor that has the strongest influence on the crystal quality. The crystal used in the diffraction experiment was selected from the experiment in which 24 mg of the dimer was dissolved in 1 cm^3 of the solvent.

Single-Crystal X-ray Diffraction. Single crystals of the dimer were obtained by slow evaporation of a CH_2Cl_2 solution as colorless elongated plates when examined separately and brownish in bulk of the material. Dimer solutions were green because, as with the majority of nitrosobenzenes, the monomer is the dominant constituent of the solution.

All diffraction experiments were performed at 100 K because the monomer phase is unstable at temperatures higher than 170 K.[7]

The single crystal of the monomer phase was obtained by irradiation of the single crystal of the dimer with a 250-W high-pressure Hg lamp for 9 h in a stream of nitrogen at 100 K while it was still mounted on the diffractometer. During irradiation, the crystal was rotated at angular speed of approximately 5°/s. The color of the crystal changed from colorless to blue/green upon irradiation.

Single-crystal data were collected on an Oxford diffraction Xcalibur 3 CCD diffractometer with graphite monochromated Mo Kα radiation. The data sets for both the dimer and the monomer phase were collected by a series of ω scans, the scan width being 1° for the dimer crystal and 2° for the monomer crystal. Scan width for the monomer crystal data collection was increased because preliminary diffraction images, taken with a 1° scan width, suggested that the quality of the crystal deteriorated as a result of the phase change. This could be seen in the spreading of reflections over a larger number of diffraction images. The data were collected up to $2\theta = 60°$ for the dimer and up to $2\theta = 50°$ for the monomer, since it diffracted very poorly at higher angles.

Both structures were solved by the Patterson method implemented in the SHELXS[10] program and refined by the least-squares method on F^2 using the SHELXL[10] program. In the dimer phase, all atoms were refined anisotropically, without any restraints, whereas for the monomer phase, anisotropic refinement of all atoms other than the bromine atom gave meaningless parameters. Anisotropic refinement with restraints on ADP resulted in no improvement of the structural data so that all the atoms, except the bromine atom, were refined isotropically. Because of rather high deviations from the expected values of the geometrical parameters of the benzene ring for the monomer phase, it was refined with some restraints on C−C bond distances. In both structures, hydrogen atoms were placed in their geometrically calculated position with the C−H bond distance of 0.93 Å and with $U_{iso}(H) = 1.2U_{eq}(C)$ for the dimer crystal and $U_{iso}(H) = 1.2U_{iso}(C)$ for the monomer crystal of the C atom to which they were bonded. All calculations were performed using the WinGX[11] crystallographic software package. Molecular structure diagrams and packing diagrams were prepared by Mercury1.3.[12] Diagrams with overlapped structures were prepared by Molekel4.3.[13]

Calculation Methods. Density functional theory (DFT)[14] calculations were carried out using the B3LYP exchange-correlation functional with the standard basis set of triple-ζ quality and with diffuse and polarization functions, namely, the 6-311+G(d,p) basis set.[15] This basis set is appropriate for systems rich in lone pairs and involved in hydrogen-bonding interactions. Population analysis of the experimentally obtained X-ray structures was performed by the natural bond orbital (NBO) method.[16] All calculations were carried out with the Gaussian 03 suite of programs,[17] and surfaces were constructed using the GaussView 3.09 visual program.

Acknowledgment. We thank Professor Emeritus D. E. Sunko for helpful discussions and comments. The financial support of the Ministry of Science and Technology, Republic of Croatia, through Grant 0119611 is gratefully acknowledged.

Supporting Information Available: S1: Crystal determination tables for structures $\mathbf{D_{ss}}$ and $\mathbf{M_{ms}2}$. S2: Single crystal determination data. S3: ORTEP diagrams of $\mathbf{D_{ss}}$ dimer and $\mathbf{M_{ms}2}$ metastable monomer. Complete crystal structure data in CIF format. S4: Powder diffraction diagram calculated on the basis of the single-crystal structure of $\mathbf{D_{ss}}$. This material is available free of charge via the Internet at http://pubs.acs.org.

JO051236U

(10) Sheldrick, G. M. *SHELXL93−Program for Crystal Structure Refinement;* Institüt für Anorganische Chemie der Universität: Göttingen, Germany, 1993.

(11) Farrugia, L. J., *J. Appl. Crystallogr*. **1999**, *32*, 837−838.

(12) Bruno, I. J.; Cole, J. C.; Edgington, P. R. Kessler, M.; Macrae, C. F. McCabe, P.; Pearson, J.; Taylor, R. *Acta Crystallogr.* **2002**, *B58*, 389−387.

(13) Kiger, P. Fl.; Thi, H. P. L.; Portmann, S.; Weber, J. Swiss Center for Scientific Computing, Manno (Switzerland), 2000.

(14) Koch, W.; Holthausen, M. C. *A Chemist's Guide to Density Functional Theory*; Wiley-VCH: Weinheim, 2000.

(15) Hehre, W. J.; Radom, L.; Schleyer, P. von R.; Pople, J. A. *Ab initio Molecular Orbital Theory*; John Wiley & Sons: New York, 1986.

(16) Jensen, F. *Introduction to Computational Chemistry*; John Wiley & Sons: Canada, 1999.

(17) *Gaussian 03*, Revision C.02; Frisch, M. J.; Trucks, G. W.; Schlegel, H. B.; Scuseria, G. E.; Robb, M. A.; Cheeseman, J. R.; Montgomery, Jr., J. A.; Vreven, T.; Kudin, K. N.; Burant, J. C.; Millam, J. M.; Iyengar, S. S.; Tomasi, J.; Barone, V.; Mennucci, B.; Cossi, M.; Scalmani, G.; Rega, N.; Petersson, G. A.; Nakatsuji, H.; Hada, M.; Ehara, M.; Toyota, K.; Fukuda, R.; Hasegawa, J.; Ishida, M.; Nakajima, T.; Honda, Y.; Kitao, O.; Nakai, H.; Klene, M.; Li, X.; Knox, J. E.; Hratchian, H. P.; Cross, J. B.; Bakken, V.; Adamo, C.; Jaramillo, J.; Gomperts, R.; Stratmann, R. E.; Yazyev, O.; Austin, A. J.; Cammi, R.; Pomelli, C.; Ochterski, J. W.; Ayala, P. Y.; Morokuma, K.; Voth, G. A.; Salvador, P.; Dannenberg, J. J.; Zakrzewski, V. G.; Dapprich, S.; Daniels, A. D.; Strain, M. C.; Farkas, O.; Malick, D. K.; Rabuck, A. D.; Raghavachari, K.; Foresman, J. B.; Ortiz, J. V.; Cui, Q.; Baboul, A. G.; Clifford, S.; Cioslowski, J.; Stefanov, B. B.; Liu, G.; Liashenko, A.; Piskorz, P.; Komaromi, I.; Martin, R. L.; Fox, D. J.; Keith, T.; Al-Laham, M. A.; Peng, C. Y.; Nanayakkara, A.; Challacombe, M.; Gill, P. M. W.; Johnson, B.; Chen, W.; Wong, M. W.; Gonzalez, C.; Pople, J. A. Gaussian, Inc.: Wallingford CT, 2004.